Chinese Journal of Natural Medicines

Identification and screening of bioactive peptides against nephropathy derived from Mantidis Otheca based on complement C3 inhibition

Shanshan Li, Peiling Liu, Tiantian Zhang, Shujun Jiang, Faren Xie, Yanliang Zhang

Citation: Shanshan Li, Peiling Liu, Tiantian Zhang, Shujun Jiang, Faren Xie, Yanliang Zhang, Identification and screening of bioactive peptides against nephropathy derived from Mantidis Otheca based on complement C3 inhibition, Chinese Journal of Natural Medicines, 2026, 24(1), 100−111. doi: 10.1016/S1875−5364(26)61080−1.

View online: https://doi.org/10.1016/S1875−5364(26)61080−1

Chinese Journal of Natural Medicines 24 (2026) 100-111

Contents lists available at ScienceDirect

Chinese Journal of Natural Medicines

journal homepage: www.cjnmcpu.com/

Original article

Identification and screening of bioactive peptides against nephropathy derived from Mantidis Oötheca based on complement C3 inhibition

Shanshan Li[a,b,c], Peiling Liu[b,c], Tiantian Zhang[b,c,d], Shujun Jiang[b,c,d], Faren Xie[b,*], Yanliang Zhang[b,c,*]

[a] *School of Pharmaceutical Sciences, Nanjing Tech University, Nanjing 211816, China*
[b] *Department of Infectious Diseases, Nanjing Hospital of Chinese Medicine Affiliated to Nanjing University of Chinese Medicine, Nanjing 210023, China*
[c] *Nanjing Hospital of Chinese Medicine Affiliated to Nanjing University of Chinese Medicine, Nanjing Research Center for Infectious Diseases of Integrated Traditional Chinese and Western Medicine, Nanjing 210006, China*
[d] *College of Engineering, China Pharmaceutical University, Nanjing 211109, China*

ARTICLE INFO

Article history:
Received 8 February 2025
Revised 11 April 2025
Accepted 27 June 2025
Available online 20 January 2026

Keywords:
Mantidis Oötheca
Nephropathy
Complement C3
Peptide screening

ABSTRACT

Insects represent emerging sources of bioactive peptides and functional materials. Mantidis Oötheca (Sang-Piao-Xiao in Chinese, SPX) serves as an insect-derived medicine for treating kidney disease. This study demonstrated that supernatant (SPX) improved kidney function in adriamycin (ADR)-induced nephropathy mice model. Transcriptomic analysis revealed that SPX inhibited complement activation by targeting the MASP1-C3/C3a receptor (C3aR) pathway. Peptidomic analysis identified 304 peptides from SPX, with 49 peptides selected for evaluation using prediction tools and molecular docking with complement core protein C3. Three peptides (PMGFPFDR, FNDPK, AAQFFNR) exhibiting docking scores below −8.0 were synthesized to verify complement inhibition and anti-fibrotic activities. The synthetic peptide AAQFFNR demonstrated complement inhibitory activity, with an inhibitory complement hemolytic 50% (ICH_{50}) value of 24.54 μmol·L^{-1}, and exhibited superior protective effects in ADR-induced HK-2 cells. Surface plasmon resonance (SPR) assay revealed direct interaction between AAQFFNR and complement C3 with K_d value of 16.8 μmol·L^{-1}. The reno-protective effect of AAQFFNR was subsequently verified in ADR-induced mice. This research provides initial evidence that complement C3-inhibiting peptides from insects demonstrate potential in preventing nephropathy through *in silico* and *in vivo* validation approaches.

1. Introduction

Chronic kidney disease (CKD) has emerged as a major public health concern, affecting more than 10% of the global population [1]. Research indicates that immunological dysfunction contributes to CKD pathogenesis, making immunosuppressive treatment the primary therapeutic approach [2]. However, steroid-induced side effects, including immune dysfunction and increased infection risk, limit treatment efficacy [3]. Consequently, the development of more effective and less toxic therapeutic interventions for CKD remains an urgent priority.

The complement system functions as an essential host defence component of innate immunity in eliminating cellular debris [4]. While its role in autoimmune disease has been recognized for over five decades, recent research demonstrates complement activation in kidney diseases not traditionally considered immune-mediated, including diabetic kidney disease and focal segmental glomerulosclerosis (FSGS) [5]. Clinical and experimental evidence indicates particular kidney vulnerability to complement-mediated inflammatory injury, with pathologies linked to abnormal complement activation. The complement system comprises three major activation pathways: classical, alternative, and lectin pathways. Complement C3, positioned at the intersection of these pathways, serves a central role in activation. Research indicates that C3 inhibition prevents its cleavage into C3a and C3b, thereby reducing downstream proinflammatory effector generation [6]. C3a interaction with C3a receptor (C3aR) triggers cellular stress and injury [7]. Furthermore, renal inflammation correlates with increased C3 expression [8]. Several complement-targeted therapeutics have received approval for kidney disease treatment, with additional anti-complement agents undergoing clinical trials [9]. Current C3 activation inhibitors, including pegcetacoplan and AMY-101, have demonstrated efficacy in C3 glomerulopathy patients [10]. Therefore, developing novel C3 inhibitors may significantly advance kidney disease treatment.

Mantidis Oötheca (mantid egg case, Sang-Piao-Xiao in Chinese, SPX), documented in Chinese Pharmacopoeia (2020 Edition) [11], represents a traditional insect medicine widely utilized in Asian countries for treating incontinence and frequent urination [12]. Contemporary pharmacological studies demonstrate SPX's anti-diuretic, anti-atherosclerotic, immunomodulatory, and fibrinolytic properties, supporting its application in preventing and treating myocardial infarction, hemorrhoids, and pediatric kidney disease [13-16]. Chemical analysis reveals that Mantidis Oötheca

* Corresponding author.
E-mail addresses: z-030133@163.com (F. Xie); fsyy00404@njucm.edu.cn (Y. Zhang)

https://doi.org/10.1016/S1875-5364(26)61080-1

contains proteins, fatty acids and phenols [17, 18]. Given its status as a traditional insect medicine, peptides likely play a crucial role in its therapeutic effects. However, limited research exists regarding its peptide constituents, and further investigation into SPX's pharmacological effects on nephropathy is warranted.

Peptidomics enables the identification of peptide components with high sensitivity, accuracy, and speed [19]. In contrast to proteomics, which studies complete proteins, peptidomics focuses on identifying peptides in specific samples, including foods, byproducts analysis, and biomarker authentication [20]. This technique is extensively utilized to identify bioactive peptides from natural plants, marine animals and fungi.

In the present study, the renal-protective effect of SPX on nephropathy was investigated both *in vivo* and *in vitro*, and complement inhibition was identified through transcriptomics and other molecular biological strategies. Peptidomics was employed to explore the bioactive peptides derived from SPX. The bioactive peptides underwent screening using molecular docking, complement inhibition test, surface plasmon resonance (SPR), and ADR-induced HK-2 cells. The peptides were synthesized *via* solid phase synthesis. ADR-induced nephropathy models both *in vivo* and *in vitro* were utilized to evaluate the peptides' activities. This study aims to identify biopeptides from traditional insect medicine and provide novel perspectives for the utility of Mantidis Oötheca.

2. Materials and methods

2.1. Chemicals and reagents

Mantidis Oötheca was obtained from the traditional Chinese medicine (TCM) market (Bozhou, China) and authenticated as *Tenodera sinensis* Saussure (Tuan-Piao-Xiao in Chinese) by Pro. Yanliang Zhang (Nanjing Hospital of Chinese Medicine Affiliated to Nanjing University of Chinese Medicine). Dried Mantidis Oötheca was processed through 60-mesh sieve to obtain powders. The powders were heated in deionized water (1∶20, *W/V*) and cooled to room temperature. The supernatant (SPX extract) was collected through centrifugation at 8000 *g*, freeze dried and stored at −80 °C until use.

Adriamycin (ADR, D107159) was obtained from Aladdin (Shanghai, China). Anti-fibronectin (Cat No. 15613-1-AP), anti-*α*-smooth muscle actin (*α*-SMA) (Cat No. 14395-1-AP), anti-collagen I (Cat No. 67288-1-Ig), anti-MASP1 (Cat No. 21837-1-AP), anti-p38 (Cat No. 14064-1-AP), anti-phosphorylated (p)-p38 (Cat No. 28796-1-AP), anti-p65 (Cat No. 66535-1-Ig), anti-p-p65 (Cat No. 82335-1-RR), anti-glyceraldehyde-3-phosphate dehydrogenase (GAPDH, Cat No. 60004-1-Ig), and HRP-conjugated goat anti-rabbit/mouse IgG (Cat No. SA00001-2, SA00001-1) were obtained from Proteintech (Wuhan, China). Anti-C3 (sc-28294), and anti-C3aR (sc-133172) were obtained from Santa Cruz (CA, USA). BCA kit (P0012) was obtained from Beyotime (Shanghai, China). Scr (C011-2-1), BUN (C013-2-1), and albumin kit (A028-2-1) were obtained from Nanjing Jiancheng (Nanjing, China). Recombinant complement C3 protein (HY-P702819) was obtained from MedChemExpress (Shanghai, China). Veronal buffer was obtained from Kejing Biological Technology Co., Ltd. (Jiangsu, China). Rabbit anti-sheep erythrocyte antibodies (Cat: H8360), 2% sheep red blood cells (SRBC, S9540) were obtained from Solarbio (Beijing, China).

2.2. Animal study

The National Institutes of Health Guidelines for the Care and Use of Laboratory Animals [SYXK (SU) 2020-0022] were followed for animal experiments. Animals were maintained under conditions at 25 °C with a 12 h/12 h light/dark cycle, and ad libitum.

Eight-week-old, 22−25 g male Balb/c mice received ADR injections (15 mg·kg^{-1}, i.v.) to induce nephropathy [21]. After model establishment, Mantidis Oötheca extract (SPX) was administered orally (100, 200, and 400 mg·kg^{-1}) for 3 weeks consecutively. For peptides, AAQFFNR was administered intravenously (10, 20, and 40 mg·kg^{-1}) daily for 3 weeks. Upon experiment completion, mice were sacrificed, and serum samples were analyzed for Scr, BUN, and albumin levels. The kidney tissues were collected for further analysis.

2.3. Histologic examination and immunohistochemical staining (IHC)

Hematoxylin and eosin (HE), Masson, and periodic acid schiff (PAS) staining were performed on 4 μm kidney slices. The sections were incubated with anti-MASP1 (1∶100) at 4 °C overnight for IHC labeling, followed by the secondary antibody and DAB dye (Zhongshan Jinqiao, Beijing, China). A Slideview VS200 microscope (Olympus, Japan) was utilized to capture the images.

2.4. Ribonucleic acid (RNA) sequencing

Total RNA was extracted from the kidney tissues. RNA purity and integrity were determined using Nanodrop 2000 (Thermo Scientific, Wilmington, DE, USA). The samples were analyzed using Illumina Novaseq 6000 (Illumina, San Diego, California, USA). For analysis, $P < 0.01$, and [Log_2 (fold change)] ≥ 2.0 were established as inclusion criteria.

2.5. Cell culture and treatment

The HK-2 cells were cultured in DMEM/F12 (Keygen, Nanjing, China) supplemented with 10% FBS (Gibco, Grand Island, NY, USA). For experiments, HK-2 cells were seeded on 6-well plates, treated with SPX extract (25, 50, and 100 μg·mL^{-1}, 1 h), and exposed to ADR (2 μg·mL^{-1}) for 24 h.

For peptides, HK-2 cells were incubated with PMGFPFDR, AAQFFNR, and FNDPR (10 μmol·L^{-1}) for 1 h, and cells were treated with ADR for 24 h.

2.6. Western blotting (WB)

Proteins were extracted from kidney tissues and cultured cells, and equal amounts of protein were separated by 10% SDS-PAGE. Following electrophoresis, proteins were transferred onto PVDF membranes. The membranes were then blocked with 5% non-fat milk in TBST and incubated overnight at 4 °C with the following primary antibodies (dilution 1∶1000 unless otherwise specified): anti-fibronectin, anti-*α*-SMA, anti-collagen I, anti-p38, anti-phospho-p38 (p-p38), anti-p65, anti-phospho-p65 (p-p65), anti-MASP1, anti-C3, anti-C3aR, and anti-GAPDH (1∶10 000). After washing, membranes were incubated with appropriate HRP-conjugated secondary antibodies (1∶10 000) for 2 h at room temperature. Protein bands were visualized using chemiluminescence and quantified using Image-Pro Plus software (version 6.0; Media Cybernetics, MD, USA)

2.7. Enzyme-linked immunosorbent assay (ELISA) detection

ELISA kits (shanghai hengyuan, Shanghai, China) were utilized to measure serum levels of tumor necrosis factor α (TNF-α,

HB050-Mu), interleukin-6 (IL-6, HS1057-Mu) and IL-1β (HB1074-Mu).

2.8. Quantitative real-time polymerase chain reaction (qRT-PCR)

1 μg of the total RNA was reversely transcribed into complementary deoxyribonucleic acid (cDNA) using a HiScriptIII RT SuperMix kit (Vazyme, Nanjing, China). The primers used for cDNA PCR amplifications were listed in Table S1.

2.9. Immunofluorescence (IF) staining

Treated cells were washed with pre-cold phosphate-buffered saline (PBS) to remove the medium, then fixed with 4% paraformaldehyde for 15 min. After three PBS washes, cells were blocked with 10% goat serum for 1 h at room temperature. The corresponding primary antibodies were then added to the cells and incubated overnight at 4 °C. After PBS washing, fluorescent secondary antibodies were added and incubated in darkness for 2 h. DAPI was added for 10 min to stain the nuclei. Images were acquired using a Zeiss microscope (Carl Zeiss, Thuringia, Germany).

2.10. Identification of SPX peptides

Peptide identification was performed following established protocols reported in the literature [22]. Briefly, 1 g of Mantidis Oötheca extract powder was suspended in SDT lysis buffer and subjected to sonication, and the resulting supernatant containing solubilized proteins was collected. Protein digestion was carried out using the FASP method [23]. The resulting peptide mixture was desalted using a C_{18}-SD extraction disk cartridge, and peptides were reconstituted in 0.1% formic acid. Peptide separation was performed using an EASY-nLC 1200 ultra-performance liquid chromatography (UPLC) system (Thermo Fisher Scientific) at a flow rate of 300 nL·min^{-1}. The mobile phases were: buffer A (0.1% formic acid in water) and buffer B (0.1% formic acid in acetonitrile). The LC gradient was programmed as follows: 0–50 min, 0–35% buffer B; 50–55 min, 35%–100% buffer B; 55–60 min, 100% buffer B.

Mass spectrometry analysis was conducted using a Q-Exactive Mass Spectrometer (Thermo Scientific, Massachusetts, USA) with the following parameters: model: positive; parent ion scanning range: *m/z* 100–1800; primary mass spectrometry resolution: 70 000 at *m/z* 200; secondary mass spectrometry resolution: 17 500 at *m/z* 200; microscans: 1; isolation window: *m/z* 2; maximum IT: 60 ms; normalized collision energy: 20 eV; dynamic exclusion: 60.0 s; underfillratio: 0.1%.

2.11. Molecular docking of the peptides with complement C3

The complement C3 structure (PDB: 2QKI) was obtained from the PDB database. Peptide structures were generated and optimized using Chem Draw and Chem 3D. Molecular docking was performed using AutoDock Vina software (Scripps Research, La Jolla, California, USA). The docking pocket grid dimensions were set to 70 × 70 × 70 (Å), with a default grid spacing of 0.375 Å. Docking results were evaluated based on docking energy, where more negative values indicated stronger binding. PyMOL software (Schrödinger, New York, USA) was used to visualize the peptide-protein complexes.

2.12. Synthesis of peptides

The three peptide sequences with the highest molecular docking scores were synthesized by Genscript (Nanjing, China) with purity exceeding 95%.

2.13. Complement inhibition

Classical pathway inhibition of the human complement system was assessed using method A described by Michaelsen et al. [24]. This assay measures the ability of a compound to inhibit complement-mediated hemolysis of SRBCs sensitized with rabbit anti-sheep erythrocyte antibodies. Diluted human serum served as the source of complement proteins. Test peptides (n = 3) were prepared in veronal buffer (Virion-Serion GmbH) and tested in duplicate at concentrations of 7.8, 15.62, 31.25, 62.5, 125, 250, 500 and 1000 μmol·L^{-1}. Each 50 μL peptide solution was mixed with 50 μL of diluted human serum in veronal buffer, pre-adjusted to achieve 50% hemolysis in the vehicle control group. The mixtures were pre-incubated for 30 min at 37 °C. Subsequently, 50 μL of 1% sensitized SRBC suspension in veronal buffer was added, followed by an additional 30-min incubation at 37 °C. After incubation, intact erythrocytes were removed by centrifugation, and the absorbance of the supernatant was measured at 405 nm using a microplate reader (Bio-Rad, USA) to quantify hemoglobin release. The percentage of hemolysis inhibition was calculated using the formula: $[(Abs_{vehicle} - Abs_{test})/Abs_{vehicle}] \times 100\%$. The concentration of each test sample required to inhibitory complement hemolytic 50% (ICH_{50}) was determined by linear interpolation. Lower ICH_{50} values indicate stronger complement inhibitory (fixation) activity

2.14. SPR

SPR assays were conducted using a Biacore X100 system (Cytiva, Massachusetts, USA). Recombinant complement C3 protein was diluted in 10 mmol·L^{-1} sodium acetate (pH 5.0, 50 μg·mL^{-1}) and immobilized on a CM5 chip (GE Healthcare, Sweden). AAQFFNR solutions at various concentrations (7.8–500 μmol·L^{-1}) were injected at 30 μL·min^{-1} across the chip surface. The interaction mode and kinetic constants between AAQFFNR and complement C3 were determined using a 1∶1 kinetic model in Biacore X100 evaluation software.

2.15. Statistical analysis

Statistical analysis was conducted using GraphPad Prism 8.0 software. All data were expressed as mean ± standard error of mean (SEM). One-way ANOVA with Dunnett's correction was employed for statistical analysis. Statistical significance was defined as P value less than 0.05.

3. Results

3.1. SPX protects against ADR-induced nephropathy in vivo

To evaluate the protective effects of Mantidis Oötheca (SPX) on kidney function, losartan (10 mg·kg^{-1}) served as a positive control. SPX (200 mg·kg^{-1}) demonstrated protective effects comparable to losartan against ADR-induced nephropathy (Fig. S1). Subsequently, doses of 100, 200, and 400 mg·kg^{-1} were selected for further investigation. Compared to the control group, ADR-induced mice exhibited significantly impaired renal function, evidenced by elevated Scr and BUN levels and decreased albumin levels (Fig. 1A). Treatment with SPX (200 and 400 mg·kg^{-1}) significantly reduced serum Scr and BUN levels while increasing albumin levels. Additionally, SPX markedly reduced the expression of fibronectin, α-SMA and collagen I (Fig. 1B). HE, MAASON and PAS staining revealed substantial ECM deposition, capsular adhesions, and vacuolar degeneration of renal tubular epithelial cells in the model group. These pathological changes were signific-

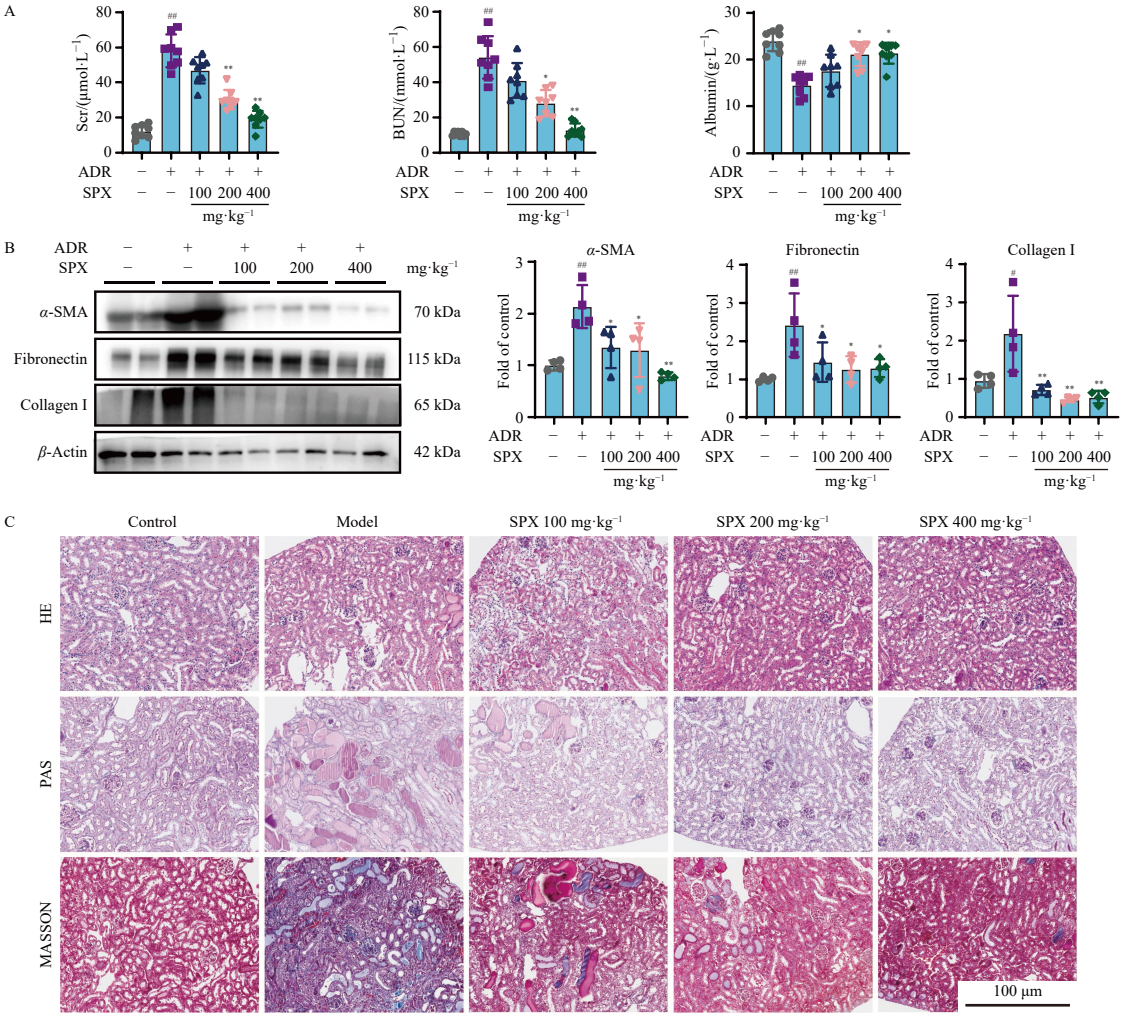

Fig. 1 SPX alleviated nephropathy in ADR-induced Balb/c mice. (A) Serum levels of Scr, BUN, and albumin in each group (n = 8). (B) The protein expressions of α-SMA, fibronectin, and collagen I in kidney tissues were analyzed by Western blotting (n = 4). (C) Representative photographs of HE, PAS, and Masson's staining from kidney tissues (scale bar: 100 μm). The data were shown as means ± SEM. $^{\#}P < 0.05$, $^{\#\#}P < 0.01$ *vs* control group; $^{*}P < 0.05$, $^{**}P < 0.01$ *vs* model group. SPX: Mantidis Oötheca extract; ADR, adriamycin.

antly ameliorated by SPX treatment (100 and 200 mg·kg^{-1}), as illustrated in Fig. 1C. These findings demonstrate that SPX extract attenuated renal fibrosis in ADR-induced mice.

3.2. SPX attenuated renal fibrosis on ADR-induced HK-2 cells

The efficacy of SPX was further investigated using ADR-induced HK-2 cells. As demonstrated in Fig. 2A, ADR treatment significantly increased the protein expression of fibronectin, α-SMA and collagen I in HK-2 cells compared to the control group. This increase was significantly reduced in cells treated with SPX (50 and 100 μg·mL^{-1}). IF staining confirmed these findings. As shown in Figs. 2B–2D, exposure of HK-2 cells to 2 μg·mL^{-1} ADR for 24 h substantially induced the expression of α-SMA, fibronectin, and collagen I, indicating extensive fibrosis in the epithelial cell cytoplasm. However, treatment with SPX at 50 μg·mL^{-1} effectively prevented ADR-mediated fibril formation.

3.3. RNA sequencing assays to identify potential pathways and genes involved in effects of SPX

To identify potential targets of SPX, RNA sequencing was performed on three groups: control, model, and SPX 200 mg·kg^{-1}. The volcano plot analysis revealed that compared with the control group, 2403 genes were upregulated and 807 genes downregulated in the ADR group. Additionally, 438 genes were upregulated and 1844 downregulated in the SPX group compared with the model group (Figs. 3A and 3B). The top 20 genes showing significant upregulation and downregulation based on fold change and P value in the kidneys are presented in Table S2. Kyoto Encyclopedia of Genes and Genomes (KEGG) pathway analysis demonstrated that TNF signaling pathway, cytokine-cytokine receptor interaction, nuclear factor κB (NF-κB) signaling pathway, and complement and coagulation cascade were the primary pathways enriched in SPX down-regulated pathways (Fig. 3C). Genes associated with these pathways exhibited increased expression in the ADR group but decreased expression in the SPX group (Figs. 3D–3G). Notably, genes involved in complement and coagulation cascade including *MASP1*, *C3*, *C3aR1*, *C1s1*, and *C1rb* showed significant upregulation in the ADR group while decreasing in the SPX group, suggesting the involvement of classical pathway and lectin pathway of complement cascade under SPX treatment. Furthermore, complement *C3* emerged as the most significantly altered gene, potentially contributing to the reno-protective effect of SPX.

3.4. SPX inhibited the complement activation both in vivo and vitro

KEGG analysis indicated the involvement of classical pathway and lectin pathway of complement cascade under SPX treatment. Previous research has demonstrated that MASP1 promotes

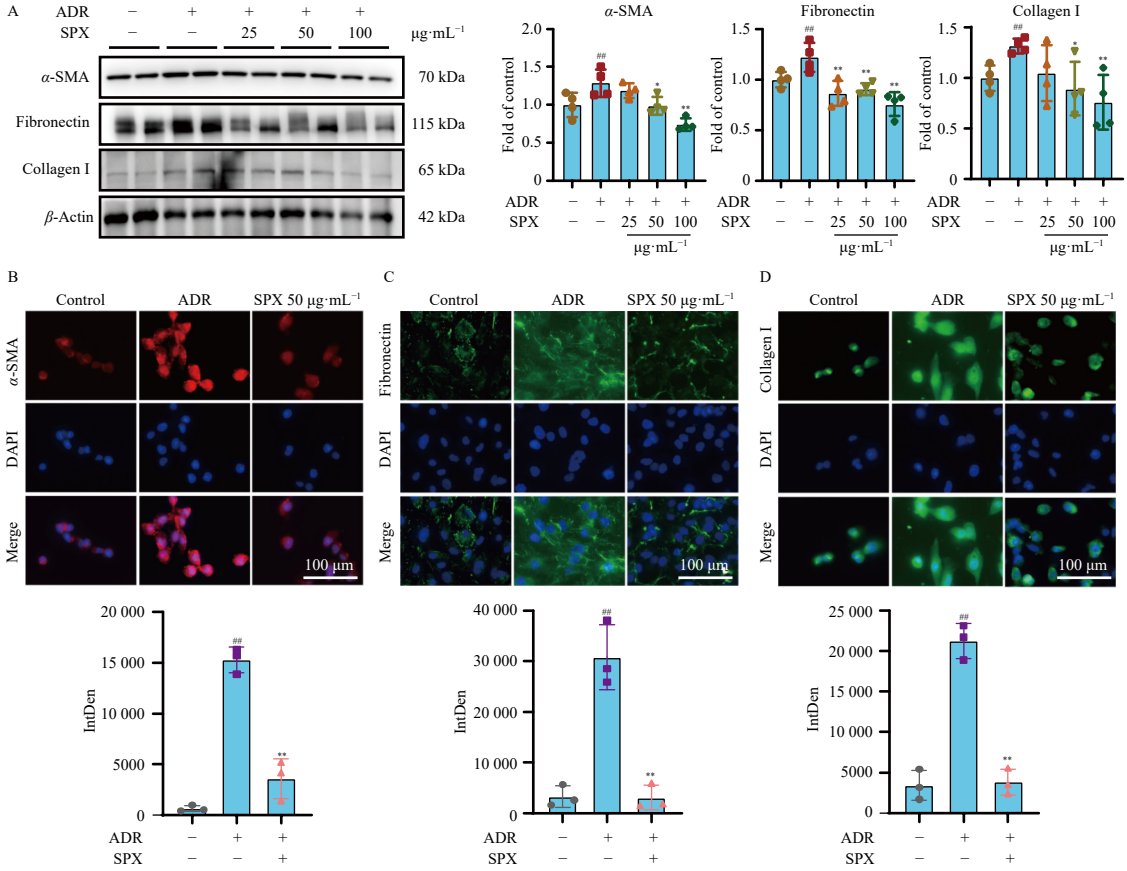

Fig. 2 Effect of SPX on ADR-induced HK-2 cells. Cells were treated with SPX (25, 50, and 100 μg·mL^{-1}) with or without ADR. (A) Protein expressions of α-SMA, fibronectin, and collagen I were analyzed by WB (n = 4). (B–D) The representative images and statistical evaluation of α-SMA, fibronectin, and collagen I detected by IF in HK-2 cells (scale bar: 100 μm; n = 3). The data were shown as means ± SEM. $^{\#}P < 0.05$, $^{\#\#}P < 0.01$ *vs* the control group; $^{*}P < 0.05$, $^{**}P < 0.01$ *vs* the model group. SPX, Mantidis Oötheca extract; ADR: adriamycin.

fibrosis through p38 mitogen-activated protein kinase (MAPK)/ATF2 signaling [25]. C3/C3aR maintains a central role in the complement pathway. Therefore, the expression of MASP1, C3 and C3aR was examined both *in vivo* and *in vitro*. As illustrated in Fig. 4A, protein levels of MASP1, C3 and C3aR increased significantly under ADR treatment. However, SPX (200 and 400 mg·kg^{-1}) substantially reduced their expression in kidney tissues. IHC analysis revealed that MASP1 was predominantly expressed in tubular cells, and SPX (200 mg·kg^{-1}) significantly decreased its expression (Fig. 4B). Consistent with WB results, IF staining demonstrated significantly increased expression of C3 and C3aR following ADR administration, while SPX treatment reduced their expression (Fig. 4C). Additionally, WB results confirmed decreased expression of MASP1, C3 and C3aR after SPX treatment in ADR-induced HK-2 cells (Fig. 4D). IF results aligned with WB findings, demonstrating SPX's inhibitory effect on C3 and C3aR expression (Fig. 4E).

3.5. SPX inhibited the inflammation through p38 MAPK-NF-κB pathway both in vivo and in vitro

The RNA sequencing results indicated significant inflammatory process involvement under SPX treatment following ADR administration. Using ELISA, the levels of TNF-α and IL-1β in mouse serum were measured. As shown in Fig. 5A, ADR significantly elevated the levels of TNF-α and IL-1β, while SPX reversed this increase in a dose-dependent manner. The messenger ribonucleic acid (mRNA) expression of *TNF-α* and *IL-1β* in kidney tissues was assessed by qRT-PCR. The results demonstrated that SPX significantly reduced *TNF-α* and *IL-1β* mRNA levels (Fig. 5B). Based on previous studies and our transcriptional analysis, the MAPK p38-NF-κB pathway plays a crucial role in inflammatory cytokine synthesis. WB was utilized to examine the protein levels of p38 MAPK, p-p38, NF-κB p65, and p-p65 in kidney tissues. As shown in Fig. 5C, the expression of p-p38 and p-p65 increased significantly in the ADR group, while SPX counteracted this elevation. Consistent with the *in vivo* results, SPX decreased the protein levels of p-p38 and p-p65 in ADR-treated HK-2 cells (Fig. 5D). The mRNA expression of *TNF-α* and *IL-1β* in HK-2 cells also decreased under SPX administration (Fig. 5E). Additionally, IF analysis revealed that ADR promoted p65 translocation from the cytoplasm to nucleus, while SPX inhibited this translocation (Fig. 5F).

3.6. Identification of bioactive peptides in SPX by peptidomics

Peptidomic analysis of SPX extract yielded 304 peptides. Multiple screening methods were implemented to identify the primary active constituents in SPX, as illustrated in Fig. 6A. Initial screening utilized PeptideRanker (distilldeep.ucd.ie/PeptideRanker/) to predict peptide bioactivity based on structural patterns, identifying 49 peptides with scores exceeding 0.5. Subsequently, docking-based virtual screening was conducted to identify potential peptide inhibitors. Given SPX's demonstrated significant inhibition of complement *C3*, which was identified as one of the most regulated genes, we hypothesized that SPX contained active peptides specifically targeting the complement C3 protein with inhibitory activity. The 49 peptides underwent molecular docking with complement C3, with scores presented in Table S3. Three peptides (PMGFPFDR, FNDPK, and AAQFFNR) with vina scores below −8.0 were identified as potential complement C3-inhibiting peptides. Their mass spectrograms and bind-

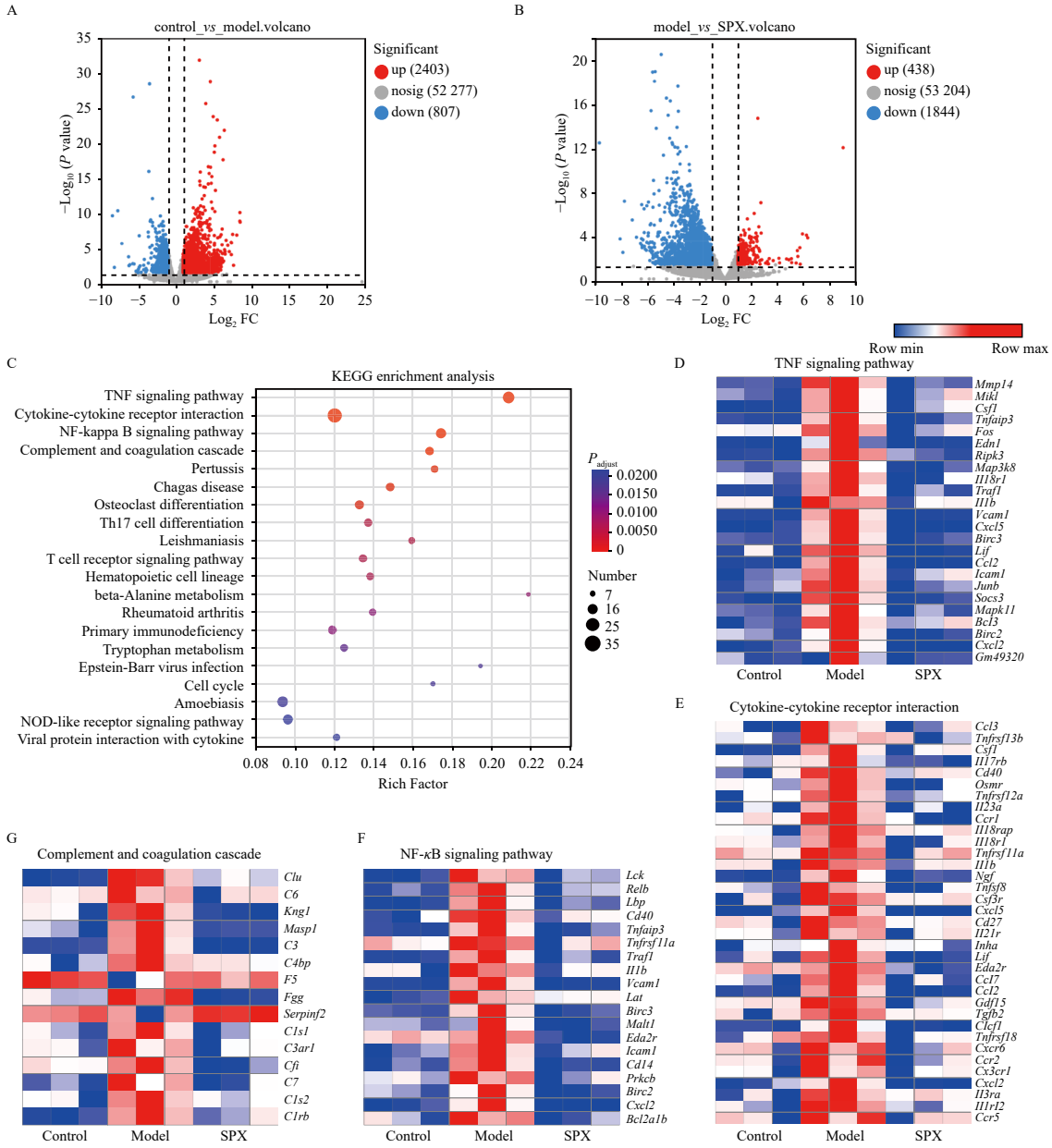

Fig. 3 RNA sequencing analysis. (A) Volcano plot of control *vs* ADR. (B) Volcano plot of ADR *vs* SPX. (C) KEGG enrichment analysis. (D) Key genes expression involved in TNF signaling pathway. (E) Key genes expression involved in cytokine-cytokine receptor interaction. (F) Key genes expression involved in NF-κB signaling pathway. (G) Key genes expression involved in complement and coagulation cascade.

ing sites with protein complement C3 are shown in Figs. 6B–6G. These peptides were synthesized and evaluated for anti-fibrotic activity in HK-2 cells. As demonstrated in Fig. 6H, AAQFFNR exhibited the most potent effects in down-regulating fibro-related proteins, suggesting its role as the primary bioactive peptide against nephropathy.

The inhibitory effects of the three peptides on human complement activation through the classical pathway were examined using NHS. As illustrated in Figs. 6I–6K, all peptides demonstrated substantial anti-complement activity. The concentrations resulting in ICH_{50} were 24.54 μmol·L^{-1} for AAQFFNR and 27.49 μmol·L^{-1} for FNDPK. In contrast, PMGFPFDR exhibited minimal activity, with an ICH_{50} value exceeding 1000 μmol·L^{-1}. Among them, AAQFFNR showed the strongest inhibitory effect on complement activation *via* the classical pathway, as indicated by its relatively low ICH_{50} value SPR assay verified the interaction between complement C3 and AAQFFNR, revealing a K_d value of 16.8 μmol·L^{-1} for direct binding, confirming AAQFFNR's direct interaction with complement C3 (Fig. 6L).

3.7. AAQFFNR preserved kidney function and reduced nephropathy induced by ADR

Given the effectiveness of AAQFFNR in reducing fibrosis, this study evaluated its therapeutic effects *in vivo*. As shown in Fig. 7A, Scr and BUN levels were elevated in mice after ADR administration but decreased following AAQFFNR treatment. ADR reduced serum albumin levels in mice, which AAQFFNR ameliorated. Serum inflammatory factors were evaluated using ELISA. As shown in Fig. 7B, AAQFFNR (20 and 40 mg·kg^{-1}) significantly reduced the levels of TNF-α, IL-6 and IL-1β. WB analysis demonstrated that AAQFFNR (20 and 40 mg·kg^{-1}) significantly decreased the expression of α-SMA, fibronectin and complement C3, respectively (Fig. 7C). Kidney fibrotic lesions were assessed through histological analysis. As shown in Fig. 7D, HE, Masson's trichrome and PAS staining revealed substantial collagen deposition, capsular adhesions, and renal tubular epithelial cell vacuolar degeneration in the model group, whereas AAQFFNR alleviated these fibrotic lesions. These results indicate that AAQFFNR

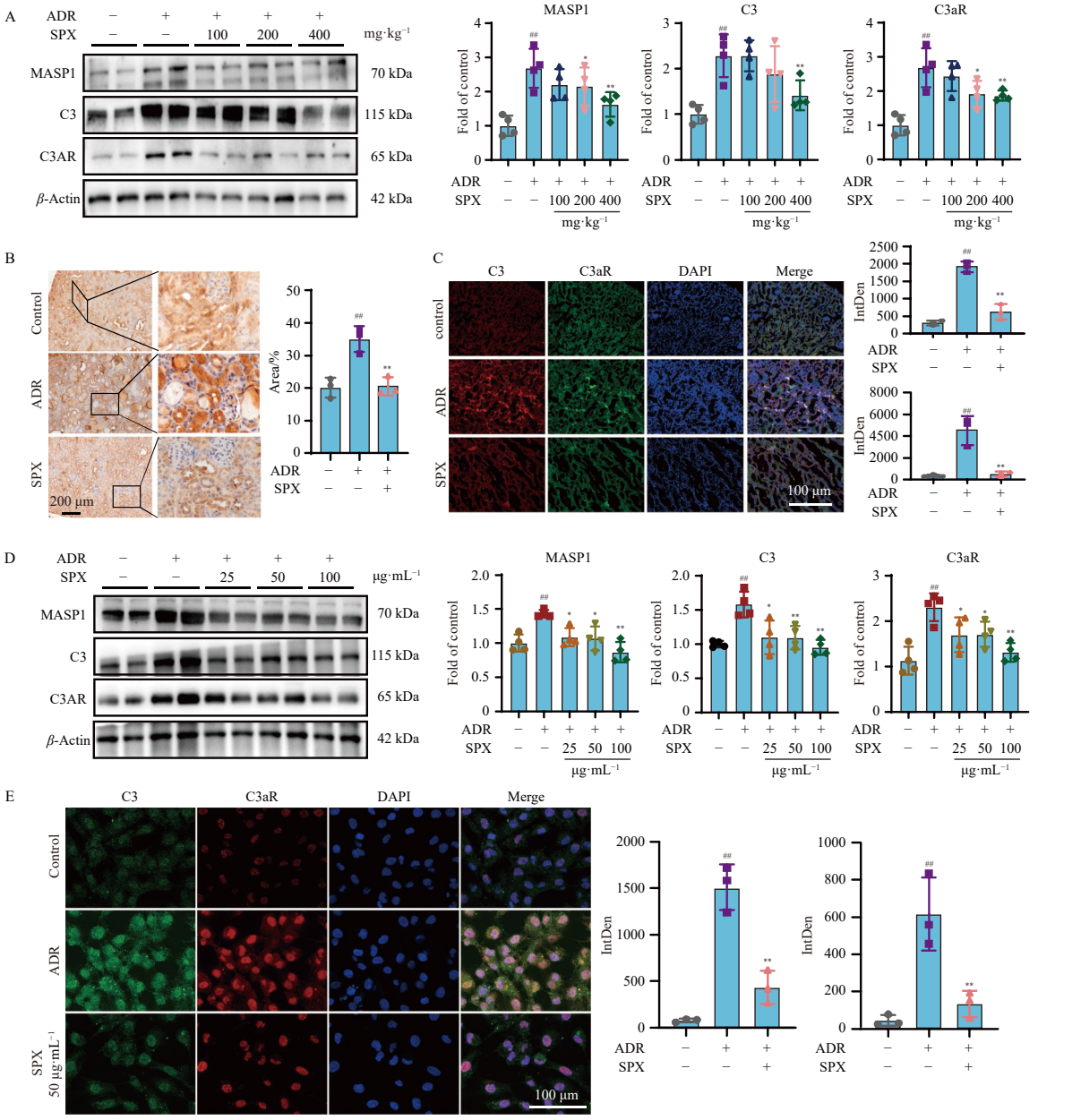

Fig. 4 SPX inhibited the complement activation *in vivo* and *in vitro* of both classical and lectin pathway. (A) The protein levels of MASP1, C3, and C3aR in kidney tissues were detected by WB (n = 4). (B) Representative IHC staining and quantitative analysis for MASP1 in kidney tissues (scale bar: 200 μm; n = 3). (C) Representative IF staining and quantitative analysis for C3 and C3aR in kidney tissues of each group (scale bar: 100 μm; n = 3). (D) The protein levels of MASP1, C3, and C3aR in ADR-induced HK-2 cells after SPX administration were analyzed by WB (n = 4). (E) The IF images quantification of C3 and C3aR in HK-2 cells (scale bar: 100 μm; n = 3). The data were shown as means ± SEM. $^{\#}P < 0.05$, $^{\#\#}P < 0.01$ *vs* control group; $^{*}P < 0.05$, $^{**}P < 0.01$ *vs* model group. SPX, Mantidis Oötheca extract; ADR, adriamycin.

ameliorated nephropathy in ADR-induced mice.

4. Discussion

The increasing incidence and mortality of CKD necessitates the development of improved treatment strategies [26]. Current therapeutic options, including ACEIs, ARBs, and SGLT2 inhibitors, have not demonstrated efficacy in delaying CKD progression [27]. Disease progression ultimately leads to ESRD, requiring renal replacement therapy [28]. TCM has been utilized for millennia in preventing and treating chronic diseases, owing to its multi-target approach and effectiveness. Beyond herbal plants, research interest has expanded to insect and marine species due to their abundant peptide constituents [29]. These peptides demonstrate diverse bioactivities with significant nutraceutical and medicinal potential [30, 31]. This study demonstrates that Mantidis Oötheca (SPX), an insect-derived medicine used clinically in Asian countries, alleviates ADR-induced nephropathy both *in vivo* and *in vitro*, showing promise for CKD treatment.

SPX, traditionally used to treat incontinence, renal failure, and leukorrhea, has demonstrated various biological activities, including anti-inflammatory, anti-diuretic, anti-cancer, and anti-oxidant properties [14]. Clinical reports indicate SPX's effectiveness in treating pediatric kidney disease and diabetic nephropathy, with significant reductions in proteinuria. However, fundamental research regarding its renal protective effects remained unexplored. This study employed an ADR-induced mouse model to simulate CKD symptoms with proteinuria [32]. Results demonstrated that SPX significantly reduced serum levels of BUN and Scr while improving kidney pathology. Similar results were observed in ADR-induced HK-2 cells. These findings suggest that SPX exhibits renal-protective effects through fibrosis inhibition.

Excessive inflammatory cytokines contribute significantly to renal inflammation and tissue damage [33]. While studies have

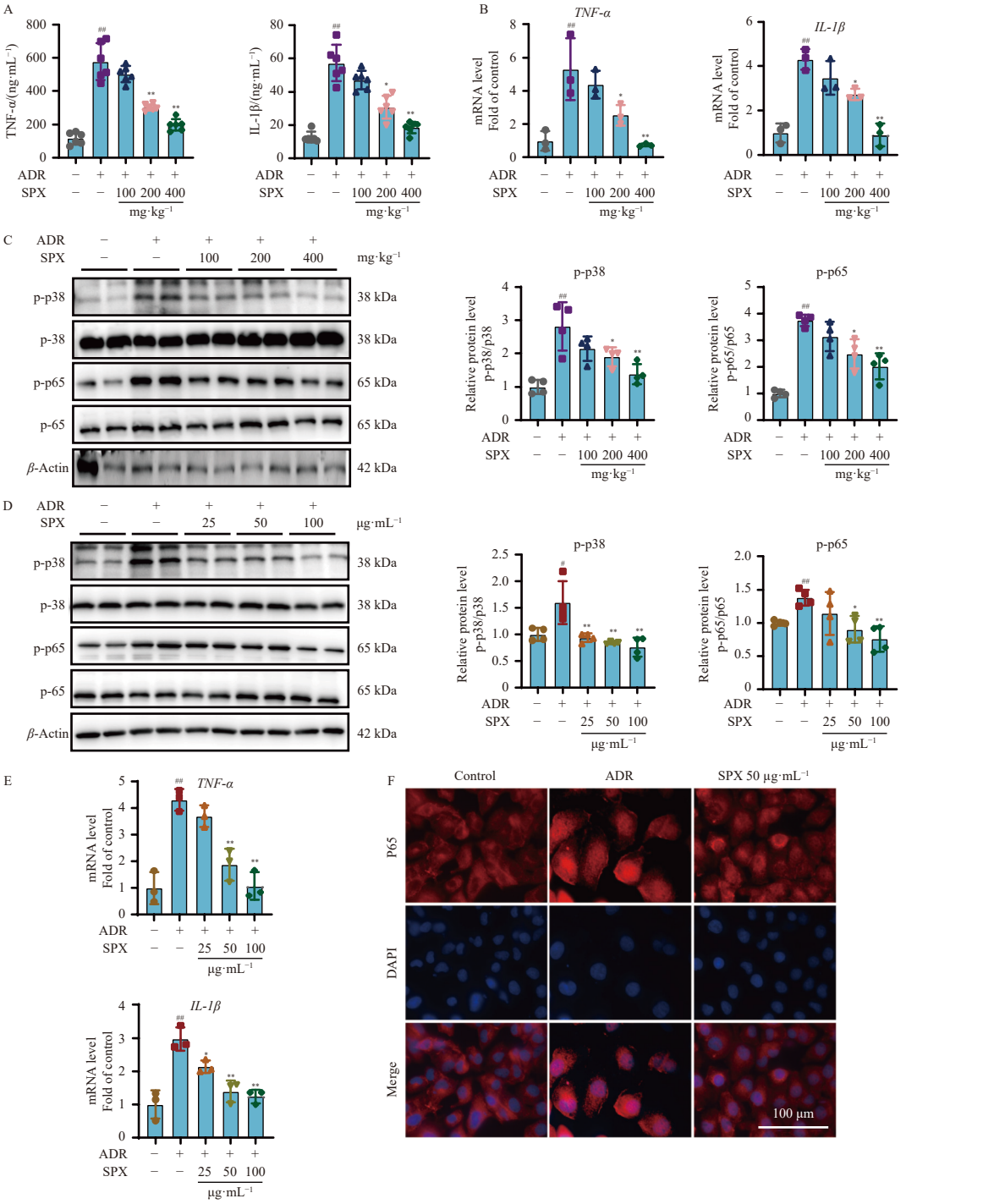

Fig. 5 SPX reduced the inflammation through p38MAPK-NF-κB pathway both *in vivo* and *in vitro*. (A) Levels of TNF-α and IL-1β in mice serum were detected using ELISA (n = 6). (B) The mRNA expression of *TNF-α* and *IL-1β* in kidney tissues were detected by qRT-PCR (n = 3). (C) The protein expressions of p38, p-p38, p65, and p-p65 in kidney tissues were analyzed by WB (n = 4). (D) The protein levels of p38, p-p38, p65, and p-p65 in ADR-induced HK-2 cells after SPX administration were analyzed by WB (n = 4). (E) The mRNA expression of *TNF-α* and *IL-1β* in HK-2 cells were detected by qRT-PCR (n = 3). (F) The representative images of p65 by IF in HK-2 cells (scale bar: 100 μm). The data were shown as means ± SEM. $^{\#}P < 0.05$, $^{\#\#}P < 0.01$ *vs* control group; $^{*}P < 0.05$, $^{**}P < 0.01$ *vs* model group. SPX, Mantidis Oötheca extract; ADR, adriamycin.

demonstrated that glomerular dysfunction represents the primary pathological factor in ADR-induced nephropathy, emerging research indicates that renal tubular cell injury also contributes substantially to renal dysfunction [34]. Damaged molecules produced by renal tubules can cause abnormal glomerular function, suggesting that tubular injury may precede glomerular dysfunction [35]. Research has shown that in ADR-induced nephrotoxicity, renal damage occurs due to persistent TNF-α accumulation [36]. IL-1β similarly plays a crucial role and leads to proximal tubule atrophy. In this study, transcriptomic analysis revealed that SPX modulated inflammation-related processes. SPX significantly reduced ADR-induced serum levels of TNF-α and IL-1β. The mRNA levels of these pro-inflammatory factors decreased in kidney tissues and HK-2 cells following SPX administration in the ADR model. P38 MAPK-NF-κB and TNF-α form a regulatory loop that amplifies inflammatory response [37]. KEGG analysis indicated that SPX significantly inhibited MAPK-NF-κB pathway activation. Since the MAPK-NF-κB pathway regulates inflammatory gene expression, the observed pro-inflammatory factor expression likely resulted from this pathway's activation [38], aligning with our findings. SPX reduced p-p38 and p-p65 protein expression without affecting p38 and p65 in ADR-treated mice. *In vitro*, SPX inhibited p65 translocation from cytoplasm to nucleus.

The complement system's abnormal activation in various

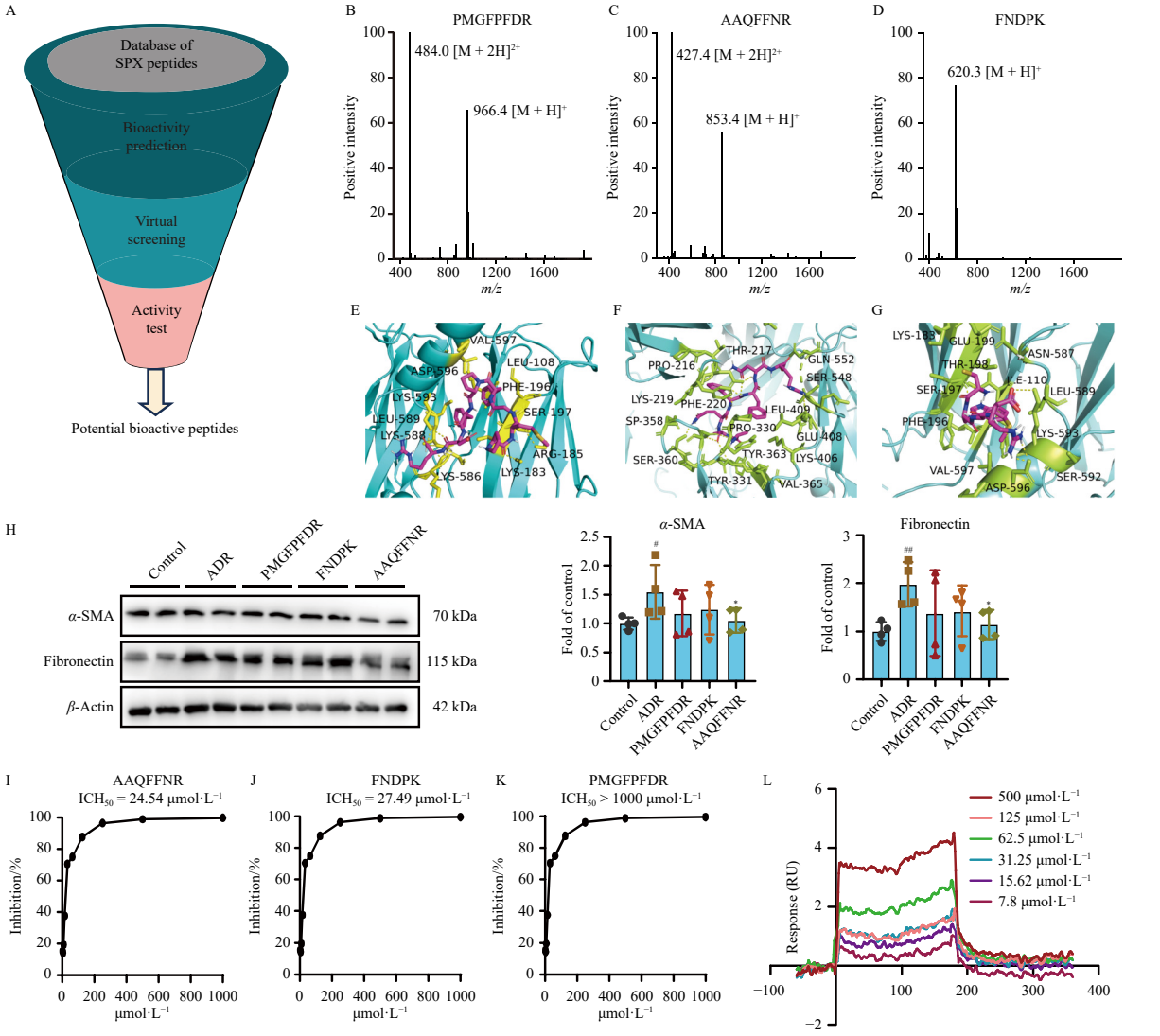

Fig. 6 Screening and verification of bioactive peptides. (A) The flow chart of activity screening. (B–D) The MS/MS spectra and structures of the peptides PMGFPFDR, AAQFFNR, and FNDPK. (E–G) Molecular docking between the peptides PMGFPFDR, AAQFFNR, and FNDPK and protein complement C3. Complement C3 was depicted in cartoon view and the peptides as stick in the binding sites. (H) HK-2 cells were pretreated with PMGFPFDR, FNDPK, and AAQFFNR (10 μmol·L^{-1}) for 1 h, and then 2 μg·mL^{-1} ADR was added for 24 h. The protein expressions of fibronectin, and α-SMA were analyzed by WB (n = 4). (I–K) Activity of the 3 peptides on the classic pathway of the complement system. (L) The interaction between complement C3 and peptide AAQFFNR. The data were shown as mean ± SEM. $^{\#}P < 0.05$, $^{\#\#}P < 0.01$ *vs* control group; $^{*}P < 0.05$, $^{**}P < 0.01$ *vs* model group.

kidney diseases indicates its significant role in renal injury pathogenesis [4]. Complement activation followed by chronic inflammation occurs in progressive CKD [5,39]. Evidence suggests that inhibiting complement activation restricts inflammation and preserves renal function [40]. Research has demonstrated that using an inhibitor of the classical and lectin pathways provided protection by reducing infiltrating cells and inhibiting endothelial-to-mesenchymal (EndMT) [41]. C3aR antagonists and C3aR gene silencing in

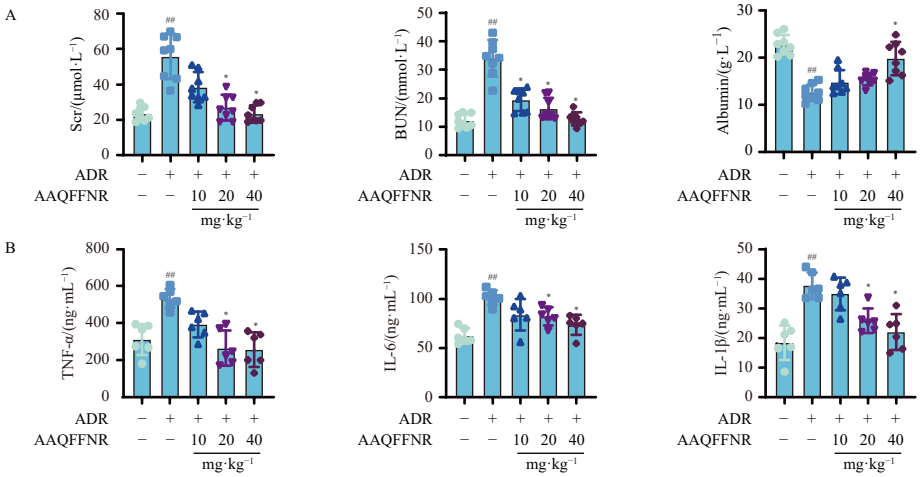

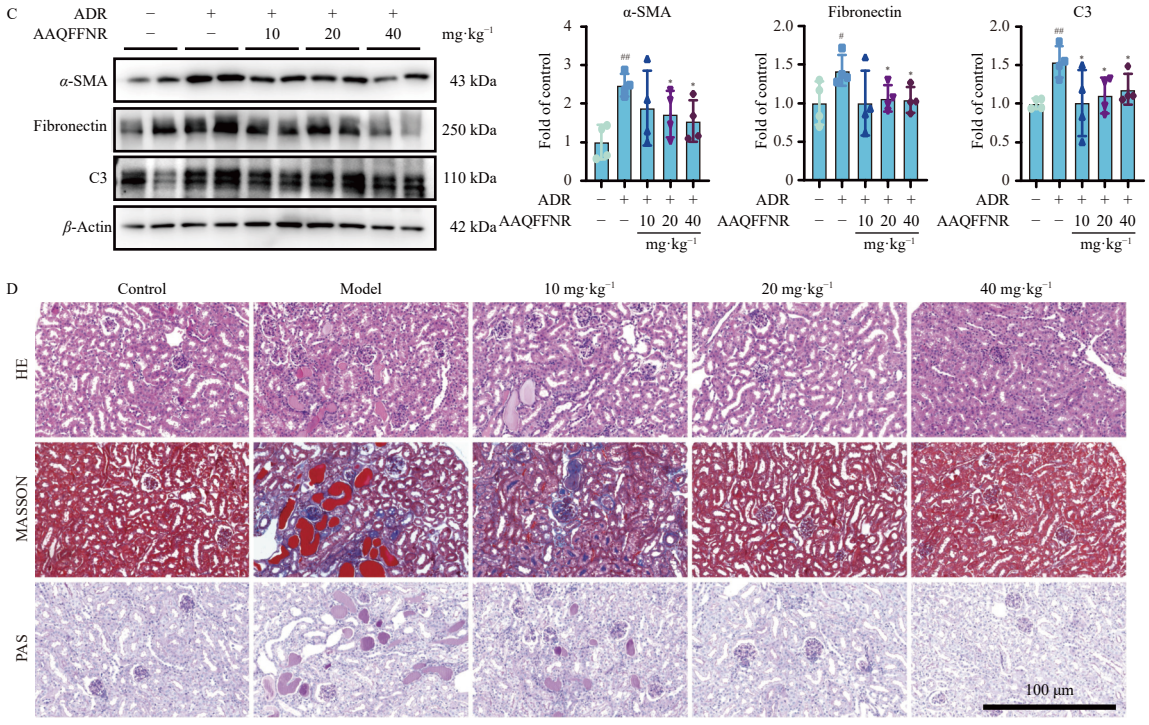

Fig. 7 Effect of peptide AAQFFNR on adriamycin-induced nephropathy. (A) Serum levels of Scr, Bun, and albumin in each group (n = 8). (B) Levels of TNF-α, IL-6 and IL-1β in mice serum were detected using ELISA (n = 6). (C) The protein expressions of α-SMA, fibronectin, and complement C3 were analyzed by WB (n = 4). (D) Representative photomicrographs of HE, PAS, and Masson's staining in kidney sections (scale bar: 100 μm). The data were shown as means ± SEM. $^{\#}P < 0.05$, $^{\#\#}P < 0.01$ *vs* control group; $^{*}P < 0.05$, $^{**}P < 0.01$ *vs* model group.

podocytes reduced oxidative stress and prevented albumin leakage [42]. MASP1-triggered pro-inflammatory factor production was regulated primarily through the p38 MAPK pathway. Regarding C3, the central protein of the complement cascade, mice receiving kidney isografts from $C3^{-/-}$ littermates showed protection against proteinuria [43]. Our RNA sequencing data indicated complement activation inhibition following SPX administration. SPX reduced MASP1, C3, and C3aR protein expression in ADR-induced mice and HK-2 cells. IHC staining demonstrated predominant MASP1 expression in tubular cells. This research suggests that SPX may achieve its therapeutic effect on nephropathy through complement activation and inflammation inhibition.

Bioactive peptides derived from natural sources demonstrate significant advantages, including high target affinity, enhanced stability, and minimal off-target effects, resulting from evolutionary chemical and structural modifications [44]. Contemporary peptidomics approaches utilizing HPLC and mass spectrometry, combined with functional prediction through *in silico* analysis, have been extensively applied to screen potential bioactive peptides from complex organisms [45]. Despite its status as a traditional Chinese insect medicine, limited research exists regarding the chemical constituents of SPX, particularly its endogenous peptides [13, 46]. This study identified 304 peptides in SPX through peptidomics analysis, representing the first systematic investigation of SPX peptide constituents. Molecular docking combined with experimental studies were employed to screen complement C3-inhibiting peptides. The structure of complement C3 comprises two chains [47]. Residues 1–534 constitute five MG domains, MG1–MG5 (MG1: residues 2–102; MG2: residues 108–202; MG3: residues 204–283; MG4: residues 329–426; MG5: residues 427–534). Residues 535–577 form one half, designated MG6b, of the b/a intertwined MG6 domain. The chain of six MG domains forms 1.5 turns of helical coil resembling a key ring. Residues 578–645 of the b-chain exit from MG6. Docking results revealed that peptide PMGFPFDR bound to C3 MG2 domains (LEU108, LYS183, ARG185, PHE196, SER197), and MG6 domains (LYS586, LYS588, LEU589, LYS593, ASP596, VAL 597). AAQFFNR bound to C3 MG3 domains (PRO216, THR217, LYS219, PHE220), MG4 domains (PRO330, TYR331, ASP358, SER360, TYR363, VAL365), and MG6 domains (SER548, GLN552). FNDPK bound to C3 MG2 domains (ILE110, LYS188, PHE196, SER197, THR198, GLU199) and MG6 domains (ASN587, LEU589, SER592, LYS593, ASP596, VAL597). Research indicates that C3 domains MG3, MG4, MG5 and MG6-8 are crucial determinants of C3 substrate recognition, and complement C3 inhibitors function by binding to native C3 and preventing its interaction with C3 convertase [48]. The complement C3 inhibitor compstatins binding site is located at the interface of MG4 and MG5 domains [49]. The differences in anti-complement activity among the three peptides may be attributed to their distinct docking sites on complement C3. Among them, AAQFFNR demonstrated the most potent anti-fibrotic activity, suggesting that its binding to the MG3 domain may play a critical role in blocking C3 activation. ICH_{50} assays confirmed the inhibitory effects of all three peptides, with AAQFFNR exhibiting the lowest ICH_{50} value, indicative of strong complement inhibition *via* the classical pathway. SPR experiments assessed AAQFFNR's binding affinity with complement C3, demonstrating direct interaction between the two molecules. This interaction provides a molecular basis for the observed complement activity inhibition in the ICH_{50} assay, highlighting AAQFFNR's potential as a lead compound for complement-targeted therapies.

5. Conclusion

In conclusion, this study employed transcriptomics, peptidomics, molecular docking, SPR, and *in vivo* and *in vitro* experiments to investigate the activities, potential mechanisms and bioactive peptides of SPX (Fig. 8). The research demonstrated that SPX ameliorated ADR-induced nephropathy through inhibition of complement C3 pathway activation. The study identified 304 peptides from SPX, with 49 peptides screened through complement C3 inhibition-based molecular docking. Docking results indicated that three peptides (PMGFPFDR, FNDPK, and AAQFFNR) formed multiple binding sites with protein C3. The *in vivo* and *in*

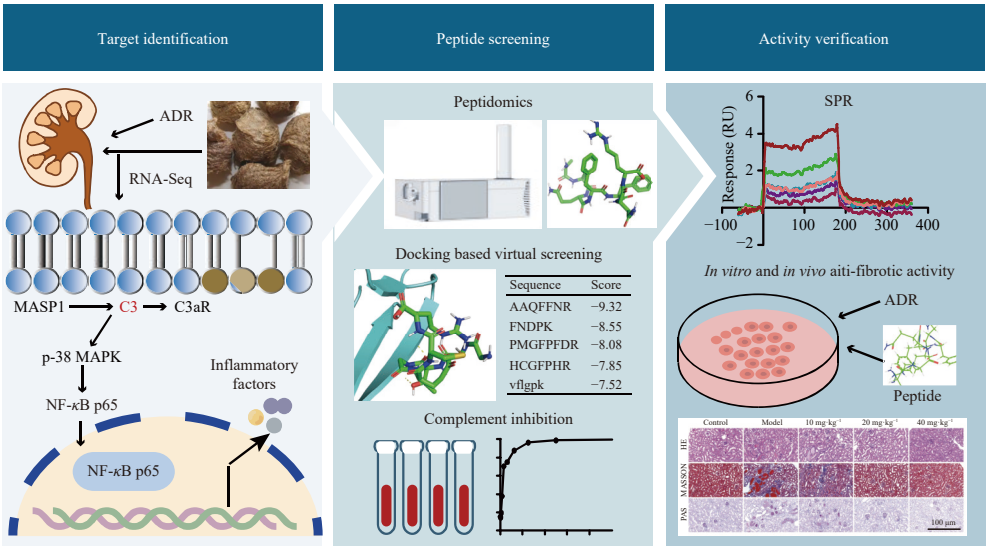

Fig. 8 Schematic diagram of potential mechanisms and bioactive peptides of Mantidis Oötheca against nephropathy.

vitro experiments established AAQFFNR as a promising functional candidate for renal failure treatment.

Funding

This work was supported by the National Natural Science Foundation of China (No. 82104353), and China Postdoctoral Science Foundation funded project (No. 2022M711680).

Supporting information

Supporting information for this study can be obtained by contacting the corresponding authors *via* E-mail.

Declaration of competing interest

The authors declare that there are no conflicts of interest.

References

1 GBD Chronic Kidney Disease Collaboration. Global, regional, and national burden of chronic kidney disease, 1990–2017: a systematic analysis for the Global Burden of Disease Study 2017. *Lancet*. 2020;395(10225):709-733. https://doi.org/10.1016/s0140-6736(20)30045-3.
2 Eddy AA, Neilson EG. Chronic kidney disease progression. *J Am Soc Nephrol*. 2006;17(11):2964-2966. https://doi.org/10.1681/ASN.2006070704.
3 Romagnani P, Remuzzi G, Glassock R, et al. Chronic kidney disease. *Nat Rev Dis Primers*. 2017;3:17088. https://doi.org/10.1038/nrdp.2017.88.
4 Fearn A, Sheerin NS. Complement activation in progressive renal disease. *World J Nephrol*. 2015;4(1):31-40. https://doi.org/10.5527/wjn.v4.i1.31.
5 Ricklin D, Reis ES, Lambris JD. Complement in disease: a defence system turning offensive. *Nat Rev Nephrol*. 2016;12(7):383-401. https://doi.org/10.1038/nrneph.2016.70.
6 Chen Y, Lin L, Rao S, et al. Complement C3 mediates podocyte injury through TLR4/NFκB-P65 signaling during ischemia-reperfusion acute kidney injury and post-injury fibrosis. *Eur J Med Res*. 2023;28(1):135. https://doi.org/10.1186/s40001-023-01054-1.
7 Gao S, Cui Z, Zhao MH. The complement C3a and C3a receptor pathway in kidney diseases. *Front Immunol*. 2020;11:1875. https://doi.org/10.3389/fimmu.2020.01875.
8 Ruseva MM, Peng T, Lasaro MA, et al. Efficacy of targeted complement inhibition in experimental C3 glomerulopathy. *J Am Soc Nephrol*. 2016;27(2):405-416. https://doi.org/10.1681/ASN.2014121195.
9 Kiss MG, Papac-Miličević N, Porsch F, et al. Cell-autonomous regulation of complement C3 by factor H limits macrophage efferocytosis and exacerbates atherosclerosis. *Immunity*. 2023;56(8):1809-1824.e10. https://doi.org/10.1016/j.immuni.2023.06.026.
10 Xu XD, Qu S, Zhang CM, et al. CD8 T cell-derived exosomal miR-186-5p elicits renal inflammation *via* activating tubular TLR7/8 signal axis. *Adv Sci*. 2023;10(25):2301492. https://doi.org/10.1002/advs.202301492.
11 Chinese Pharmacopoeia (Part I). China: Medical Science Press; 2020.
12 Song JH, Cha JM, Moon BC, et al. Mantidis oötheca (mantis egg case) original species identification *via* morphological analysis and DNA barcoding. *J Ethnopharmacol*. 2020;252:112574. https://doi.org/10.1016/j.jep.2020.112574.
13 Ryu SM, Nam HH, Kim JS, et al. Chemical constituents of the egg cases of *Tenodera angustipennis* (*Mantidis ootheca*) with intracellular reactive oxygen species scavenging activity. *Biomolecules*. 2021;11(4):556. https://doi.org/10.3390/biom11040556.
14 Zand AM, Saadati M, Zargan J. Active components of mantis eggs and their immunomodulatory effect in a mouse model. *Biologia*. 2019;74(1):45-51. https://doi.org/10.2478/s11756-018-0111-9.
15 Walker AA, Weisman S, Kameda T, et al. Natural templates for coiled-coil biomaterials from praying mantis egg cases. *Biomacromolecules*. 2012;13(12):4264-4272. https://doi.org/10.1021/bm301570v.
16 Wang J, Guo X, Zou Z, et al. *Ootheca mantidis* mitigates renal fibrosis in mice by the suppression of apoptosis *via* increasing the gut microbe *Akkermansia muciniphila* and modulating glutamine metabolism. *Biomed Pharmacother*. 2023;166:115434. https://doi.org/10.1016/j.biopha.2023.115434.
17 Hahn BS, Cho SY, Wu SJ, et al. Purification and characterization of a serine protease with fibrinolytic activity from *Tenodera sinensis* (praying mantis). *Biochim Biophys Acta*. 1999;1430(2):376-386. https://doi.org/10.1016/s0167-4838(99)00024-2.
18 Hahn BS, Cho SY, Ahn MY, et al. Purification and characterization of a plasmin-like protease from *Tenodera sinensis* (Chinese mantis). *Insect Biochem Mol Biol*. 2001;31(6-7):573-581. https://doi.org/10.1016/s0965-1748(00)00162-4.
19 Purohit K, Reddy N, Sunna A. Exploring the potential of bioactive peptides: from natural sources to therapeutics. *Int J Mol Sci*. 2024;25(3):1391. https://doi.org/10.3390/ijms25031391.
20 Maes E, Oeyen E, Boonen K, et al. The challenges of peptidomics in complementing proteomics in a clinical context. *Mass Spectrom Rev*. 2019;38(3):253-264. https://doi.org/10.1002/mas.21581.
21 Wang Y, Wang YP, Tay YC, et al. Progressive adriamycin nephropathy in mice: sequence of histologic and immunohistochemical events. *Kidney Int*. 2000;58(4):1797-1804. https://doi.org/10.1046/j.1523-1755.2000.00342.x.
22 Zhang M, Zhu L, Zhang H, et al. Virtual screening of GLP-1-secreting peptides from Pea protein hydrolysates *via* peptide transporter 1 (PepT1) activation-based molecular docking. *J Agric Food Chem*. 2024;72(24):13646-13653. https://doi.org/10.1021/acs.jafc.4c00999.
23 Tremblay TL, Hill JJ. Adding polyvinylpyrrolidone to low level protein samples significantly improves peptide recovery in FASP digests: an inexpensive and simple modification to the FASP protocol. *J Proteomics*. 2021;230:104000. https://doi.org/10.1016/j.jprot.2020.104000.
24 Di H, Zhang Y, Chen D. An anti-complementary polysaccharide from the roots of *Bupleurum chinense*. *Int J Biol Macromol*. 2013;58:179-185. https://doi.org/10.1016/j.ijbiomac.2013.03.043.
25 Liu X, Tan S, Liu H, et al. Hepatocyte-derived MASP1-enriched small extracellular vesicles activate HSCs to promote liver fibrosis. *Hepatology*. 2023;77(4):1181-1197. https://doi.org/10.1002/hep.32662.
26 Ruiz-Ortega M, Rayego-Mateos S, Lamas S, et al. Targeting the progression of chronic kidney disease. *Nat Rev Nephrol*. 2020;16(5):269-288. https://doi.org/10.1038/s41581-019-0248-y.
27 Chevalier RL. Evolution, kidney development, and chronic kidney disease. *Semin Cell Dev Biol*. 2019;91:119-131. https://doi.org/10.1016/j.semcdb.2018.05.024.
28 Perazella MA. Drug use and nephrotoxicity in the intensive care unit. *Kidney Int*. 2012;81(12):1172-1178. https://doi.org/10.1038/ki.2010.475.
29 Muttenthaler M, King GF, Adams DJ, et al. Trends in peptide drug discovery. *Nat Rev Drug Discov*. 2021;20(4):309-325. https://doi.org/10.1038/s41573-020-00135-8.
30 Craik DJ, Fairlie DP, Liras S, et al. The future of peptide-based drugs. *Chem Biol Drug Des*. 2013;81(1):136-147. https://doi.org/10.1111/cbdd.12055.
31 Geng Q, Sun X, Gong T, et al. Peptide-drug conjugate linked *via* a disulfide bond for kidney targeted drug delivery. *Bioconjug Chem*. 2012;23(6):1200-1210. https://doi.org/10.1021/bc300020f.
32 Lee VW, Harris DC. Adriamycin nephropathy: a model of focal segmental

glomerulosclerosis. *Nephrology (Carlton)*. 2011;16(1):30-38. https://doi.org/10.1111/j.1440-1797.2010.01383.x.
33 Li S, Yang Q, Chen F, et al. The antifibrotic effect of pheretima protein is mediated by the TGF-β1/Smad2/3 pathway and attenuates inflammation in bleomycin-induced idiopathic pulmonary fibrosis. *J Ethnopharmacol*. 2022;286:114901. https://doi.org/10.1016/j.jep.2021.114901.
34 Ferenbach DA, Bonventre JV. Kidney tubules: intertubular, vascular, and glomerular cross-talk. *Curr Opin Nephrol Hypertens*. 2016;25(3):194-202. https://doi.org/10.1097/MNH.0000000000000218.
35 Tan RJ, Li Y, Rush BM, et al. Tubular injury triggers podocyte dysfunction by *β*-catenin-driven release of MMP-7. *JCI Insight*. 2019;4(24):e122399. https://doi.org/10.1172/jci.insight.122399.
36 He LY, Niu SQ, Yang CX, et al. Cordyceps proteins alleviate lupus nephritis through modulation of the STAT3/mTOR/NF-*κ*B signaling pathway. *J Ethnopharmacol*. 2023;309:116284. https://doi.org/10.1016/j.jep.2023.116284.
37 Tao X, Li J, He J, et al. *Pinellia ternata* (Thunb.) Breit. attenuates the allergic airway inflammation of cold asthma *via* inhibiting the activation of TLR4-medicated NF-*κ*B and NLRP3 signaling pathway. *J Ethnopharmacol*. 2023;315:116720. https://doi.org/10.1016/j.jep.2023.116720.
38 Zhang Y, Li Z, Wu H, et al. Esculetin alleviates murine lupus nephritis by inhibiting complement activation and enhancing Nrf2 signaling pathway. *J Ethnopharmacol*. 2022;288:115004. https://doi.org/10.1016/j.jep.2022.115004.
39 Gao S, Cui Z, Zhao MH. Complement C3a and C3a receptor activation mediates podocyte injuries in the mechanism of primary membranous nephropathy. *J Am Soc Nephrol*. 2022;33(9):1742-1756. https://doi.org/10.1681/ASN.2021101384.
40 Vivarelli M, Barratt J, Beck LH, et al. The role of complement in kidney disease: conclusions from a kidney disease: improving global outcomes (KDIGO) controversies conference. *Kidney Int*. 2024;106(3):369-391. https://doi.org/10.1016/j.kint.2024.05.015.
41 Xu L, Xu H, Chen S, et al. Inhibition of complement C3 signaling ameliorates locomotor and visual dysfunction in autoimmune inflammatory diseases. *Mol Ther*. 2023;31(9):2715-2733. https://doi.org/10.1016/j.ymthe.2023.07.017.
42 Zhang Q, Bin S, Budge K, et al. C3aR-initiated signaling is a critical mechanism of podocyte injury in membranous nephropathy. *JCI Insight*. 2024;9(4):e172976. https://doi.org/10.1172/jci.insight.172976.
43 Sheerm NS, Risley P, Abe K, et al. Synthesis of complement protein C3 in the kidney is an important mediator of local tissue injury. *FASEB J*. 2008;22(4):1065-1072. https://doi.org/10.1096/fj.07-8719com.
44 Adermann K, John H, Ständker L, et al. Exploiting natural peptide diversity: novel research tools and drug leads. *Curr Opin Biotechnol*. 2004;15(6):599-606. https://doi.org/10.1016/j.copbio.2004.10.007.
45 Dallas DC, Guerrero A, Parker EA, et al. Current peptidomics: applications, purification, identification, quantification, and functional analysis. *Proteomics*. 2015;15(5-6):1026-1038. https://doi.org/10.1002/pmic.201400310.
46 Noh S, Kim WJ, Cha JM, et al. Rapid diagnostic PCR assay method for species identification of *Mantidis ootheca* (Sangpiaoxiao) based on cytochrom C oxidase I (COI) barcode analysis. *Int J Mol Sci*. 2024;25(18):10224. https://doi.org/10.3390/ijms251810224.
47 Forneris F, Ricklin D, Wu J, et al. Structures of C3b in complex with factors B and D give insight into complement convertase formation. *Science*. 2010;330(6012):1816-1820. https://doi.org/10.1126/science.1195821.
48 Janssen BJC, Huizinga EG, Raaijmakers HCA, et al. Structures of complement component C3 provide insights into the function and evolution of immunity. *Nature*. 2005;437(7058):505-511. https://doi.org/10.1038/nature04005.
49 Lamers C, Xue X, Smieško M, et al. Insight into mode-of-action and structural determinants of the compstatin family of clinical complement inhibitors. *Nat Commun*. 2022;13(1):5519. https://doi.org/10.1038/s41467-022-33003-7.